Liquid Crystals
Publication details, including instructions for authors and subscription information:
http://www.informaworld.com/smpp/title~content=t713926090

Dynamic light scattering from liquid crystal polymer brushes swollen in a nematic solvent

Farida Benmouna; Bin Peng; Jacek Gapinski; Adam Patkowski; Jürgen Rühe; Diethelm Johannsmann

Online publication date: 06 August 2010

To cite this Article Benmouna, Farida , Peng, Bin , Gapinski, Jacek , Patkowski, Adam , Rühe, Jürgen and Johannsmann, Diethelm(2001) 'Dynamic light scattering from liquid crystal polymer brushes swollen in a nematic solvent', Liquid Crystals, 28: 9, 1353 — 1360
To link to this Article: DOI: 10.1080/02678290110061395
URL: http://dx.doi.org/10.1080/02678290110061395

LIQUID CRYSTALS, 2001, VOL. 28, NO. 9, 1353–1360

Dynamic light scattering from liquid crystal polymer brushes swollen in a nematic solvent

FARIDA BENMOUNA†‡, BIN PENG†, JACEK GAPINSKI§,
ADAM PATKOWSKI†§, JÜRGEN RÜHE†
and DIETHELM JOHANNSMANN†*

†Max-Planck-Institute for Polymer Research, Ackermannweg 10, 55128, Mainz, Germany

‡Permanent address: Faculty of Sciences, University Aboubakr Belkaid, Tlemcen BP 119, Algeria

§Institute of Physics, A. Mickiewicz University, Umultowska 85, 61-614, Poznan, Poland

(*Received 21 November 2000; accepted 27 March 2001*)

Surface-attached side group liquid crystal polymer monolayers ('brushes') swollen in a nematic solvent were studied by means of dynamic light scattering. In the temperature range 47.5–66°C, the swollen brush is nematic while the bulk liquid crystal is isotropic. Under these conditions the light scattering is dominated by the brush. The fluctuations in the brush are 1–2 orders of magnitude slower than the fluctuations in the bulk nematic. The autocorrelation functions are well fitted by Kohlrausch–Williams–Watts stretched exponentials of the form $\exp[(-t/\tau)^{\beta}]$ with a dynamic exponent β in the range 0.6–0.8.

1. Introduction

Polymer surfaces swollen in their environment are very interesting objects with regard to their structure, their dynamical behaviour, and the function they may carry [1]. A particular class of such interfaces are tethered layers, which consist of surface-attached linear polymer chains. For high graft densities, neighbouring chains overlap ('polymer brushes') and the chains stretch away from the surface [2, 3]. In good solvents, polymer brushes swell and are very soft [4].

In liquid crystal (LC) polymer brushes the LC director field introduces additional complexity into the system [5]. LC orientation is of particular interest when the adjacent phase is a low molecular mass nematic liquid crystal. In this case, the LC orientation at the polymer surface may be transferred into the bulk phase and the polymer can act as an alignment layer. Such alignment layers are key elements in liquid crystal displays [6–8]. Naturally, this possibility has attracted some interest. Hikmet has described in some detail the use of surface-attached gel phases of liquid crystal polymers (LCPs) as alignment layers [9]. Although the interaction of the bulk phase with the gel surface in general may be complicated, the gel layer provides design flexibility in terms of the chemical structure and the degree of crosslinking.

*Author for correspondence;
e-mail: johannsmann@mpip-mainz.mpgde

In the case of LCP brushes, vertical chain stretching plays a special role. If, for example, the mesogenic side groups of a side group LCP brush are preferentially aligned perpendicular to the main chain, the nematic director will be parallel to the substrate. If, on the other hand, the graft density is low and the main chains lie flat on the surface, forming a 'pancake', the nematic director will be perpendicular to the interface. In addition, the ordering influence of the polymer chains may compete with a second, different orienting force originating from the uncovered portions of the substrate [10, 11].

In this work we report dynamic light scattering measurements on LCP brushes in contact with their low molecular mass analogues. According to the 'grafting-from' approach, the polymer chains were grown *in situ* by free radical chain polymerization from initiator molecules which were covalently attached to the surface [12, 13]. A laterally homogeneous orientation can be achieved by strongly rubbing the substrate with a nylon cloth prior to the immobilization of the initiator [14]. For the light scattering measurements, we have focused on temperatures between 47.5 and 66°C. In this range the swollen brush is nematic while the solvent is isotropic and, as a consequence, the scattering from the nematic brush by far outweighs the scattering from the isotropic bulk.

Fytas and other workers have previously investigated the dynamics of terminally anchored polymer layers

Liquid Crystals ISSN 0267-8292 print/ISSN 1366-5855 online © 2001 Taylor & Francis Ltd
http://www.tandf.co.uk/journals
DOI: 10.1080/02678290110061395

with evanescent dynamic light scattering. From the thermal fluctuations of the segment density profile these authors inferred the dynamic behaviour of the 'breathing mode' [15–17]. In the depolarized light scattering experiment, orientation fluctuations of optically anisotropic samples are measured. For nematic liquid crystals these fluctuations result in a much higher scattered intensity than density fluctuations. The strength of the scattering mechanism is impressively demonstrated by the fact that one can collect depolarized light scattering data under conditions where only the 60 nm thick brush contributes to scattering. In this case the effective scattering volume is a factor of 1000 smaller than in regular '3D' experiments. The high scattering efficiency in the VH configuration made our experiments much easier compared with evanescent light scattering, which entails problems in the analysis because the scattering vector becomes complex. On the other hand, the underlying modes of fluctuations are more complicated.

In addressing the dynamic fluctuations in the brush, we must first ask the question, to what extent is the brush indeed 'soft'. We argue that the mere existence of dynamic fluctuations proves that the brush is swollen. With regard to the application of the LCP brush as an alignment layer for LC cells, the dynamic properties of the brush will clearly enter the dynamic behaviour of the bulk liquid crystal as a boundary condition. The dynamics of the interface affects the dynamic response of the entire cell.

2. Director fluctuations in polymer brushes

In nematic liquid crystals fluctuations of the orientation and concomitant fluctuations of the dielectric tensor are the dominant source of light scattering [18, 19]. The formalism developed for low molecular mass nematics also holds, in principle, for polymer liquid crystals [20–22]. In a well aligned sample the mesogenic molecules are on average oriented parallel to the preferred direction given by the director $\mathbf{n}_0$. The instantaneous local orientation fluctuates around the average orientation by a small amount, $\delta\mathbf{n}(\mathbf{r}, t)$. The concomitant fluctuations of the dielectric tensor, $\delta\varepsilon(\mathbf{r}, t)$, strongly scatter light.

In the bulk the eigenmodes of the orientation fluctuations are given by exponentially decaying harmonic waves. The intensity autocorrelation function, $G^{(2)}(\mathbf{q}, t)$, of the scattered light is proportional to the autocorrelation function of the dielectric constant fluctuations, $I^{\varepsilon}_{\mathrm{if}}(\mathbf{q}, t)$, given by [23]

$$I^{\varepsilon}_{\mathrm{if}}(\mathbf{q}, t) = \lim_{T\to\infty} \frac{1}{T} \int_{t_0}^{t_0+T} \mathrm{d}t' \delta\varepsilon^{*}_{\mathrm{if}}(\mathbf{q}, t') \delta\varepsilon_{\mathrm{if}}(\mathbf{q}, t'+t) \quad (1)$$

where $\mathbf{q}$ is the scattering vector, and t is the autocorrelation time. The asterisk denotes the complex conjugate. $\delta\varepsilon_{\mathrm{if}}(\mathbf{q}, t)$ is given by the integral

$$\delta\varepsilon_{\mathrm{if}}(\mathbf{q}, t) = \int_V \mathrm{d}^3 r \exp(\mathrm{i}\mathbf{q}\mathbf{r}) \mathbf{n}_{\mathrm{f}} \;\; \delta\varepsilon(\mathbf{r}, t) \;\; \mathbf{n}_{\mathrm{i}}. \quad (2)$$

Here V is the scattering volume, $\mathbf{n}$ is the polarization vector, and the indices i and f denote the initial and the final state, respectively. In the bulk, the quantity $\delta\varepsilon_{\mathrm{if}}(\mathbf{q}, t)$ is the Fourier transform of $\mathbf{n}_{\mathrm{f}} \;\; \delta\varepsilon(\mathbf{r}, t) \;\; \mathbf{n}_{\mathrm{i}}$. Scattering in a given direction is caused by the individual Fourier components, the Fourier components being at the same time the eigenmodes of the orientation fluctuations.

In tethered LCP layers the situation is more complex because the system is inherently heterogeneous in space. The boundary conditions strongly come into play [24]. Also, the sample thickness is comparable to the wavelength of light and the integration over the scattering volume no longer amounts to a Fourier transform [25]. Strictly speaking, the integration over the vertical spatial component amounts to a discrete Fourier transform with very poor sampling. Due to these complications we do not attempt a rigorous quantitative analysis of our data. However, some general statement about the nature of the fluctuations may be made.

Perpendicular to the substrate plane, the scattering volume is of the same order of magnitude as q_z^{-1}. If the thickness is much less than q_z^{-1} (for example because the scattering vector is in the sample plane, see configuration A in figure 1), the situation is simplified because one can use the relation $\exp(\mathrm{i}q_z z) \approx 1$. Along the z-coordinate the scattering amplitude turns into an integral over the director fluctuations. In this case the scattering is dominated by the mode with the lowest gradients along z satisfying the boundary conditions. The higher order modes have nodal planes in the brush, and the integral leads to a partial cancellation between regions with an opposite sign of $\delta\mathbf{n}(z)$. Also, the modes with low gradients are least expensive in terms of the elastic free energy and therefore have the largest thermal excitation amplitudes.

The boundary conditions at the bottom of brush are known. The easy axis is the rubbing direction identified here with the x-axis. Although we have not measured the anchoring strength, it seems reasonable to assume 'strong anchoring' in the sense that the director is pinned at the bottom of the brush [26]. This assumption is corroborated by our finding that randomly aligned dry brushes have a strong surface memory effect [13, 27]. The anchoring conditions at the brush–bulk interface are degenerate with regard to the azimuthal angle corresponding to twist distortions. With regard to the polar angle (corresponding to a splay–bend distortion of the brush), there may be a preferred angle and a non-zero anchoring

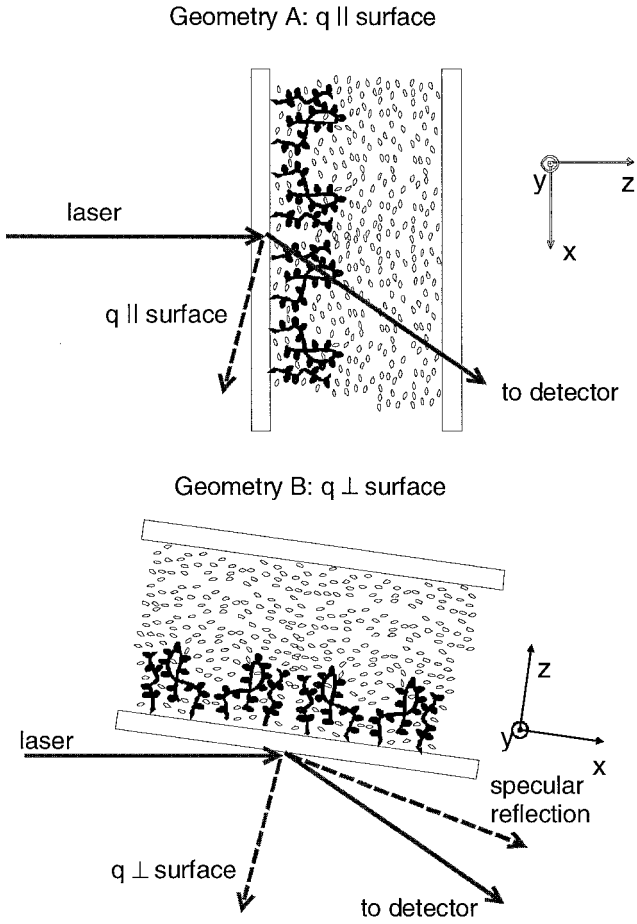

Figure 1. Geometries chosen for the DLS measurements. In both cases the detector was placed 35° away from the transmitted beam. In geometry A the sample was perpendicular to the incident beam, while in geometry B the sample was tilted away from normal incidence by 80°.

energy. The degree to which the bend distortion contributes to scattering depends on the scattering angle. The bend contribution is small for a scattering vector perpendicular to the nematic director (geometry B in figure 1). Bend contributions couple to shear flow, which is much suppressed in brushes.

As we will see, the observed correlation functions in most cases cannot be described by single exponentials. On a heuristic basis, we fitted the data with Kohlrausch–Williams–Watts stretched exponentials of the form

$$G^{(2)}(t) - 1 \approx A \exp\left[-\left(\frac{t}{\tau}\right)^{\beta}\right] \qquad (3)$$

where $G^{(2)}(t)$ is the intensity autocorrelation (AC) function as measured with the correlator, τ is the decay time, and $\beta \leqslant 1$ is the dynamic exponent. For mono-exponential decays β is close to 1. A dynamic exponent of $\beta < 1$ is frequently encountered in polymer physics [28]. A is the amplitude of the correlation function

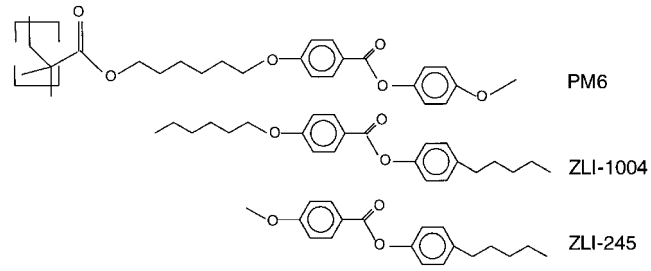

Figure 2. Chemical structure of the side group liquid crystal polymer PM6 forming the brush and the low molecular mass components ZLI-1004 and ZLI-245. The nematic solvent ZLI-1052 is a 2:1 eutectic mixture of ZLI-1004 and ZLI-245.

ranging between 0 and 1. The amplitude A is less than 1 in the case of heterodyne detection where a static and a dynamic scattering signal are superimposed. In our experiments the imperfect alignment and substrate roughness always introduced some static background. The static background varied significantly over the sample surface and further depended on the sample state. Imperfect alignment causes strong static scattering when the sample is in the nematic state. In the isotropic state, this source of scattering vanishes just like the dynamic fluctuations of the nematic director. The contrast of the correlation function A depends on the ratio of the intensity scattered by the ordered liquid crystalline sample to the intensity of the static background.† For example, A drops sharply around the bulk N–I transition temperature, $T_{\mathrm{NI,bulk}} = 47.5°\mathrm{C}$, because the entire cell scatters below $T_{\mathrm{NI,bulk}}$ while only the brush contributes significantly above the bulk clearing temperature. The intensity of the light scattered in the completely isotropic state ($T > 66°\mathrm{C}$) was negligible compared with the scattering below 66°C.

3. Materials and sample preparation

Figure 2 depicts the chemical structure of the LCP brush and the bulk nematic solvent. Details of the synthesis which followed the 'grafting-from' technique are provided in [13]. The surface-attached monolayers of the polymer PM6 were grown *in situ* from a covalently grafted initiator layer. The phenylbenzoate mesogenic side groups are linked to the poly(methyl methacrylate)-backbone via a flexible hexyl spacer. Polymerization was carried out at 60°C in toluene. The substrate was a BK7 glass slide (Schott, Mainz, Germany). The thickness of the investigated brushes was around 65 nm in the dry

† Very *fast* relaxations which are not resolved by the correlator, for instance caused by the reorientation of individual molecules, would have the same effect as a static background. Strictly speaking, the amplitude A is given by the ratio of the amplitudes of scattering inside and outside the experimental time window.

state as measured with a profilometer. The brushes were aligned along the *x*-axis, i.e. along the scattering plane, by rubbing the substrate prior to polymer growth [14].

The low molecular mass LC material (kindly provided by Merck KGaA) has the code ZLI-1052. It is a eutectic mixture of the two phenylbenzoate derivatives ZLI-1004 and ZLI-245 shown in figure 2. Unfortunately, liquid crystal polymers are often poorly miscible with their low molecular weight analogues [29]. Since the mesogenic molecules are larger than conventional solvent molecules, the intermolecular cohesive forces are large and the relative importance of the mixing entropy is low. In a previous study, we have investigated the miscibility of the bulk side group LCP PM6 with its low molecular weight analogue ZLI-1052 by differential scanning calorimetry and optical microscopy [30]. At room temperature there is an extended miscibility gap ranging from a very small polymer fraction to a polymer content of about 50%, see figure 3(*a*). Around 65°C the gap narrows and shifts towards higher polymer concentration; it vanishes at the N–I transition temperature of the pure polymer. This phase diagram implies that at room temperature the brush can only swell to about twice its dry thickness. At the upper edge of the brush there is a phase boundary where the polymer concentration rapidly drops from about 50% to close to zero, figure 3(*b*).

The light scattering experiments were carried out on liquid crystal cells with a thickness of about 30 μm. The thickness was adjusted with Mylar spacers between the two microscope slides forming the cell. Only one cell surface was coated with a brush; the other surface was rubbed with a peice of teflon in order also to provide alignment along the *x*-axis. The cells were filled with ZLI-1052 by capillary action at room temperature. After filling, the cell was sealed with a UV-curable glue (B651-0 from Bohle, Haan, Germany). The glue did not deteriorate in the index matching fluid (*trans*-decalin) over a duration of 11 h at 100°C.

In one experiment the brush was replaced by a spin-cast film of the same polymer as the brush. This material was prepared from the same monomer, and the initiator was dissolved in the bulk, rather than being immobilized on the glass surface. The molecular weight was 156 000 g mol^{-1} with a polydispersity index, $M_w/M_n \sim 3.85$. The thickness of the spin-cast layer was 100 nm as measured with a profilometer. The director of the spin-cast film was also aligned along the rubbing direction of the substrate.

4. Experimental

Dynamic light scattering (DLS) measurements were performed using an ALV goniometer (ALV, Langen, Germany). We used a frequency-doubled 200 mW

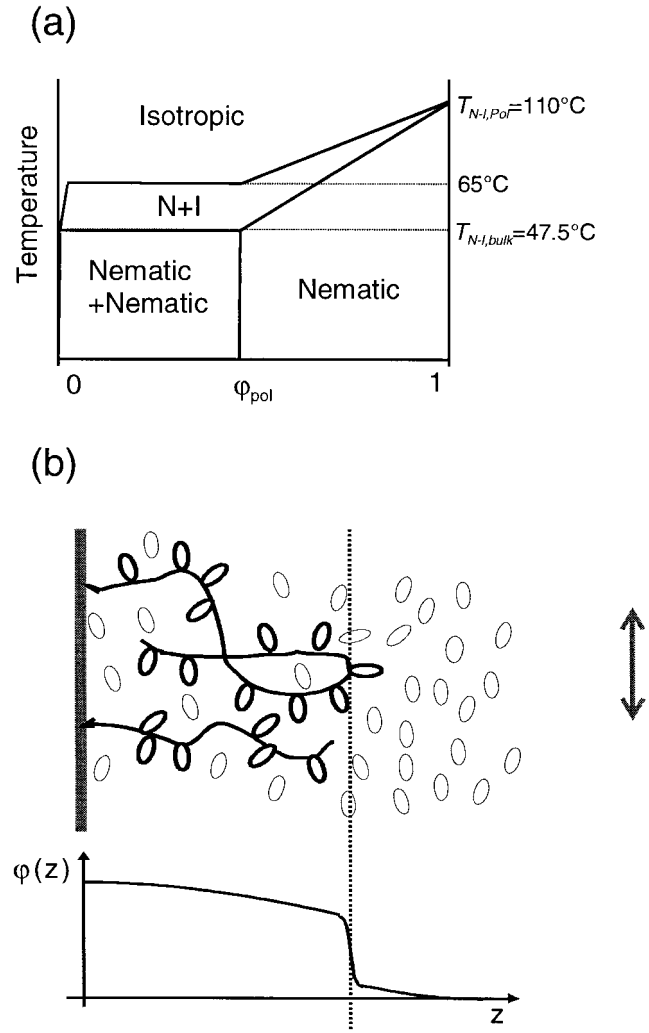

Figure 3. (*a*) Schematic representation of the phase diagram of the polymer/ZLI-1052 mixture. φ_{pol} is the polymer volume fraction. (*b*) Sketch of the phase boundary at the brush/LC interface: a meniscus separates the swollen brush and the almost pure low molecular mass nematic phase.

Nd-YAG laser (ADLAS, Germany) with a wavelength of $\lambda = 532$ nm. When working on the bulk nematic, attenuating filters were inserted into the beam to reduce the count rate of the scattered light to less than 100 kHz. For measurements on the brushes, for which the count rate was low, all filters were removed. We used crossed polarizers so that only the depolarized component of the scattered light was detected. We observed no effects of laser-induced heating. The sample was immersed into a cylindrical cuvette fitting the goniometer; it could be translated and rotated with a special holder. The cylindrical cuvette was filled with *trans*-decalin to provide thermal contact with the thermostat. Moreover, the refractive index of *trans*-decalin closely matches that of glass, reducing static scattering from the outer cell

surface. The thermostat controlled the temperature to within 0.1°C. Optical fibres were used to collect the scattered light. The detector was an avalanche diode connected to an ALV-5000 digital correlator (ALV, Langen, Germany); the correlator measures the intensity autocorrelation function $G^{(2)}(t)$.

We used two different scattering geometries, A and B as shown in figure 1. In geometry A the incoming beam hits the sample with vertical incidence. The detector was placed at an angle of 35° away from the transmitted beam. The scattering vector in this case had a magnitude of 10.6 μm^{-1} and made an angle of 17.5° with the sample plane. In geometry B the sample was inclined with respect to the incoming beam. We placed the detector as close as possible to the specular reflection, resulting in close-to-perpendicular orientation of the scattering vector with respect to the sample plane. The scattering vector had a magnitude of 10.6 μm^{-1} and made an angle of 82.5° with respect to the sample surface.

5. Results and discussion

Figure 4 shows two autocorrelation functions displaying the general phenomenology. Both data traces were obtained on a cell with a 65 nm brush in contact with the bulk solvent in geometry A. At temperatures below the clearing temperature of the bulk nematic, 47.5°C, we found autocorrelation functions dominated by the bulk. The decay curves are single exponentials and look similar to the decay curves found for ZLI-1052 on bare glass slides. When raising the temperature to above 47.5°C the picture is significantly different. Firstly, the amplitude of the autocorrelation function drops, indicating a decrease in the dynamic scattering intensity relative to the static background; while the entire cell contributes to scattering below the bulk N–I transition temperature, only the brush contributes above. Secondly, the time constants for the decay are much larger for the brush; apparently, the polymer main chains considerably slow down the processes of relaxation. Also, the decay is no longer given by a single exponential but rather by a stretched exponential of the form $A \exp[(-t/\tau)^{\beta}]$ with a dynamic exponent β less than 1. We attempted to fit the data with biexponentials but could find no solutions with an acceptable margin of error. In figures 5 and 6 we show the fitting parameters τ, β, and A as a function

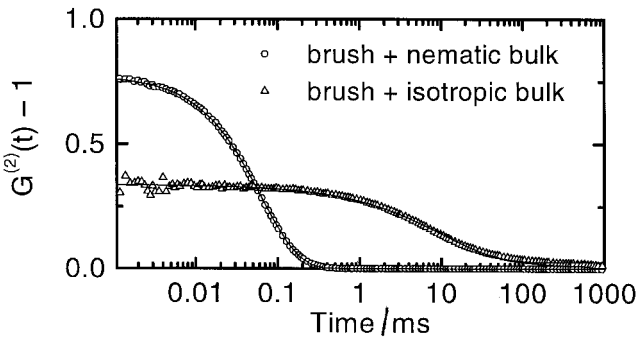

Figure 4. Autocorrelation functions taken in geometry A below 45°C (○) and above 62°C (△). The bulk N–I temperature is 47.5°C. The solid lines represent fits with stretched exponentials according to $G^{(2)}(t) - 1 \approx A \exp[(-t/\tau)^{\beta}]$.

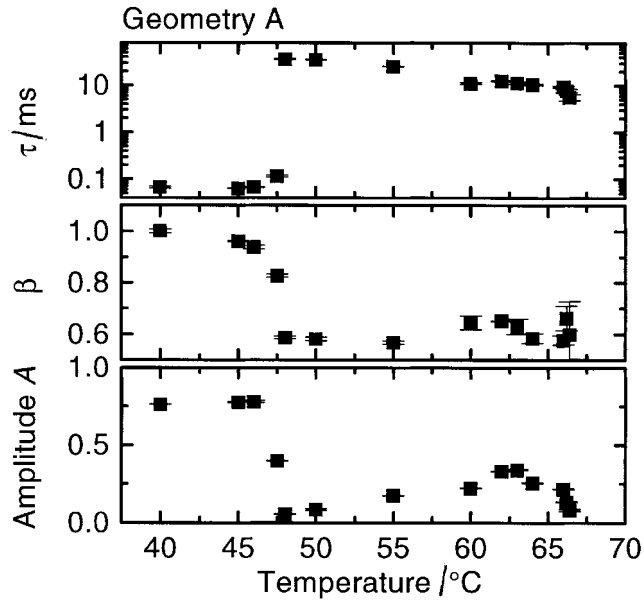

Figure 5. Decay times τ, dynamical exponents β, and scattering amplitudes A as a function of temperature obtained in geometry A.

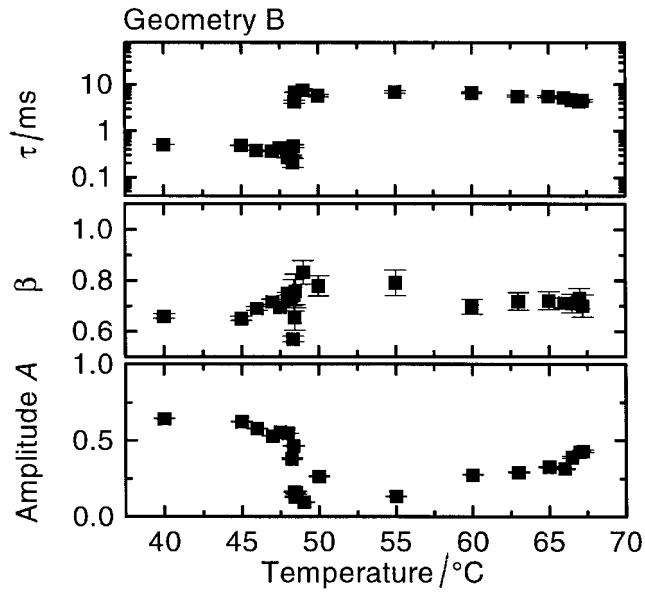

Figure 6. Decay times τ, dynamical exponents β, and scattering amplitudes A as a function of temperature obtained in geometry B.

of temperature for the two scattering geometries A and B. In geometry B the bulk has a longer decay time and a smaller coefficient β than in geometry A. Above the N–I transition temperature of the bulk the general behaviour is rather similar in the two geometries. The decay time decreases with increasing temperature, presumably due to a decrease of viscosity with temperature. The dynamic coefficient β does not vary much with temperature. The scattering amplitude A shows some variation; however, A is affected by the static background, which is difficult to control.

Figure 7 shows the autocorrelation functions as the temperature is slowly increased through the bulk N–I transition temperature. When keeping the sample at a nominal temperature of 47.5°C there is a slow evolution with time. The true temperature at the sample spot increases very slowly. At intermediate times we find a distinctly bimodal decay curve. We attribute the slow and the fast component to the brush and to a thin wetting layer of the nematic solvent, respectively. Because the wetting layer contains very little polymer, it shows fast fluctuations. Such prewetting behaviour is expected because the brush and the bulk nematic are chemically similar [31]. Figure 8 shows an optical micrograph obtained on a similar cell close to the bulk N–I transition temperature, corroborating the prewetting interpretation. The bright circular regions are nematic droplets in an isotropic matrix. In addition to these droplets one observes a bright region with a diffuse boundary at the bottom of the micrograph. Interference fringes indicate that the thickness of this prewetting layer at the brush surface increases continuously from top to bottom. The fast dynamic component in figure 7 originates from such a nematic layer decreasing in thickness with time.

In figure 9 we show data sets gathered around the N–I transition temperature of the swollen brush at 66°C. According to the phase diagram from [30], figure 3(*a*),

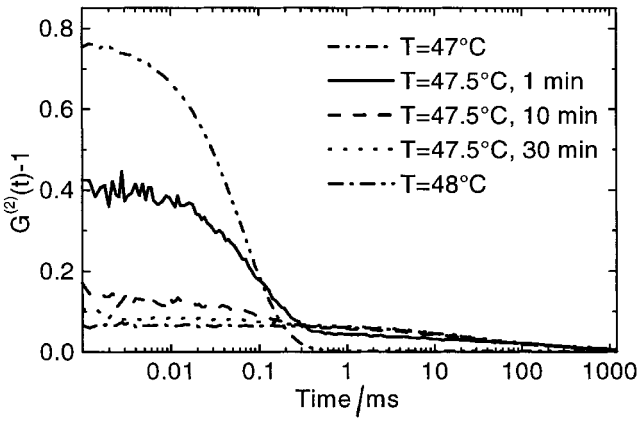

Figure 7. Autocorrelation functions measured close to the transition temperature of the bulk.

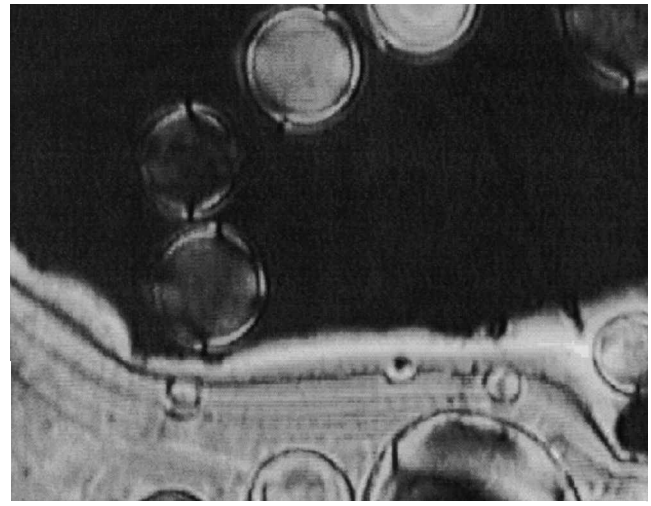

Figure 8. Micrographs of a cell showing prewetting behaviour. The field of view corresponds to about 100 μm.

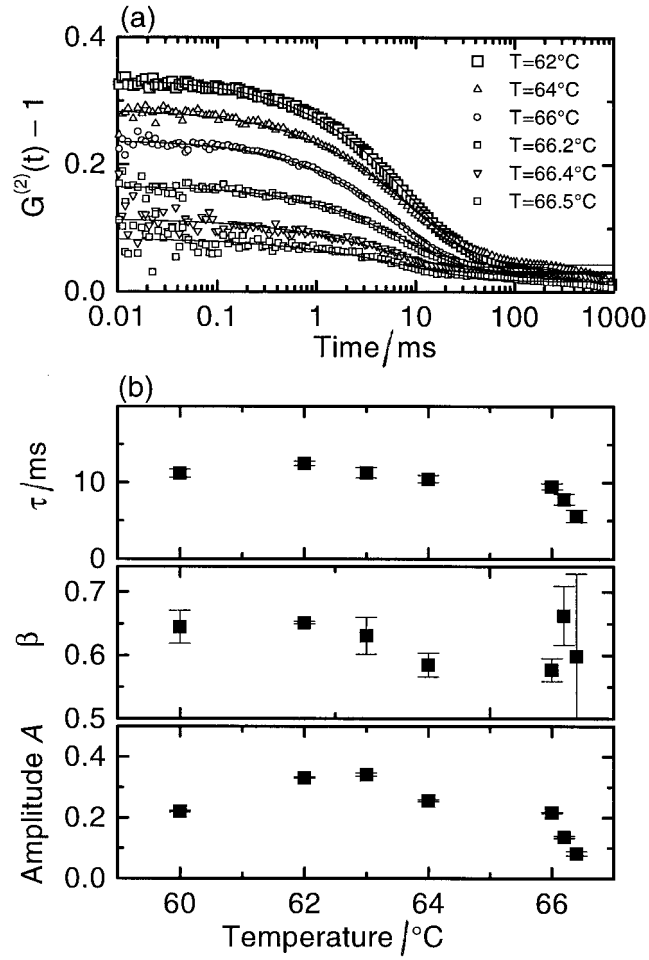

Figure 9. (*a*) Autocorrelation functions obtained in geometry A close to the transition temperature of the swollen brush of 66°C. (*b*) Fitting parameters as a function of temperature.

this transition temperature indicates that the swollen brush contains about 50% nematic solvent. Presumably, there is a composition gradient from the top to the bottom of the brush resulting in a rather broad transition range of 0.5°C. As the temperature increases the nematic sheet gradually becomes thinner until the isotropic phase hits the substrate. As figure 9 (*a*) shows, the amplitude A gradually decreases with increasing temperature. At the same time, the decay time decreases because the reorientation becomes faster as the nematic layer thins out. The coefficient β remains essentially unchanged.

Finally, we investigated the question of whether the dynamic exponent $\beta < 1$ is an effect related to polymer dynamics in a very general sense, or whether it is a consequence of the terminal attachment of the chains at the bottom of the brush. Gu and co-workers have worked on bulk side group LCPs in nematic solvents and found monoexponential decays, despite the presence of the polymer chains [22]. As figure 10 shows we also find monoexponential decays when working on a spin-cast polymer layer instead of a polymer brush. While both dry and wet brushes yield stretched exponentials with $\beta \sim 0.6$–0.7, the swollen spin-cast liquid crystal polymer shows an almost purely monoexponential decay with $\beta > 0.95$. We conclude that the broad distribution of relaxation times found for brushes relates to the fact that the polymer chains are covalently tethered to the substrate. Interestingly, the breathing modes in swollen polystyrene brushes observed by Fytas and co-workers also showed monoexponential relaxation dynamics [15]. It should be noted, however, that the dynamic behaviour of LC-brushes is much richer than the behaviour of semidilute isotropic brushes, because the director field can transmit a torque between different chains. A direct comparison of the dynamics of isotropic and liquid crystalline brushes is problematic.

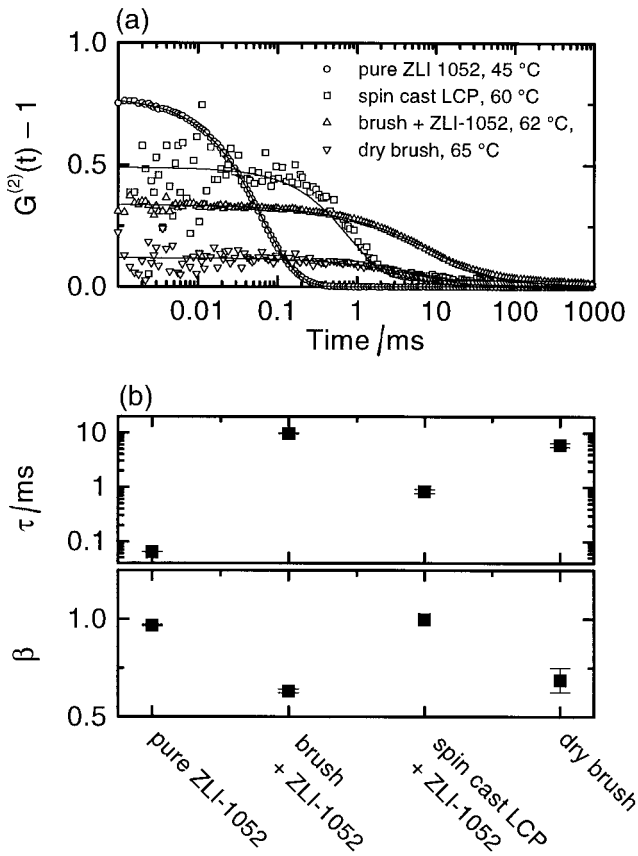

Figure 10. (*a*) Comparison of the dynamic behaviour in geometry A of the pure nematic solvent, a swollen brush, a swollen spin-case film of the polymer PM6, and a dry brush at the temperatures indicated in panel. (*b*) Fitting parameters for the various samples.

6. Conclusions

The depolarized light scattering from liquid crystalline polymer brushes is so strong that it easily allows one to probe the dynamical behaviour of 60 nm thick specimens with conventional DLS equipment. The decay times of the autocorrelation functions were in the millisecond range and decreased with increasing temperature. Just above the bulk N–I transition temperature of 47.5°C, a thin nematic solvent layer prewets the nematic brush. The N–I transition of the brush has a width of about 0.5°C, which is attributed to a polymer concentration gradient perpendicular to the substrate. The autocorrelation functions decay according to stretched exponentials with a dynamic exponent β in the range 0.6–0.8. A comparison with spin-cast films shows that the low dynamic exponent β is related to the covalent attachment of the chains to the substrate.

F. Benmouna thanks Professor W. Knoll for his kind invitation to the MPI-P where this work has been accomplished.

References

[1] Fleer, G. J., Cohen Stuart, M. A., Scheutjens, J. M. H. M., Cosgrove, T., and Vincent, B., 1993, *Polymers at Interfaces* (Chapman and Hall).
[2] Milner, S. T., 1991, *Science*, **251,** 905.
[3] Halperin, A., 1991, *Adv. Polym. Sci.*, **100,** 31.
[4] Klein, J., 1996, *Annu. Rev. Mater. Sci.*, **26,** 581.
[5] Amoskov, V. M., Birshtein, T. M., and Pryamitsyn, V. A., 1996, *Macromolecules*, **29,** 7240.
[6] Cognard, J., 1982, *Alignment of Liquid Crystals and their Mixtures* (Gordon and Breach).
[7] Demus, D., 1990, in *Liquid Crystals and Uses*, edited by B. Bahadur (World Scientific).
[8] Crawford, G. P., and Zumer, S., (editors), 1996, *Liquid Crystals in Complex Geometries Formed by Polymers and Porous Networks* (Taylor and Francis).
[9] Hikmet, R. A. M., 1992, *Adv. Mat.*, **4,** 679.

[10] Halperin, A., and Williams, D. R. M., 1993, *Europhys. Lett.*, **21,** 575.
[11] Halperin, A., and Williams, D. R. M., 1994, *J. Phys. Condens. Mat. A*, **297,** 6.
[12] Prucker, O., and Rühe, J., 1998, *Macromolecules*, **31,** 592.
[13] Peng, B., Johannsmann, D., and Rühe, J., 1999, *Macromolecules*, **32,** 6759.
[14] Peng, B., Johannsmann, D., and Rühe, J., 2000, *Adv. Mat.* **12,** 821.
[15] Fytas, G., Anastasiadis, S. H., Seghrouchni, R., Vlassopoulos, D., Li, J., Factor, B. J., Theobald, W., and Toprakcioglu, C., 1996, *Science*, **274,** 2041.
[16] De Gennes, P. G., 1992, *Adv. Colloid Interface Sci.*, **27,** 189.
[17] Farago, B., Monkenbusch, M., Richter, D., Huang, J. S., Fetters, L. J., and Gast, A. P., 1993, *Phys. Rev. Lett.*, **71,** 1015.
[18] De Gennes, P. G., and Prost, J., 1993, *The Physics of Liquid Crystals* (Oxford University Press).
[19] Forster, D., Lubensky, T., Martin, P., Swift, J., and Pershan, P., 1971, *Phys. Rev. Lett.*, **26,** 1016.
[20] Gu, D., Jamieson, A. M., Kawasumi, M., Lee, M.-S., and Percec, V., 1992, *Macromolecules*, **25,** 2151.
[21] Gu, D., and Jamieson, A. M., 1991, *Mol. Cryst. liq. Cryst.*, **209,** 147.
[22] Gu, D., Jamieson, A. M., Rosenblatt, C., Tomazos, D., Lee, M.-S., and Percec, V., 1991, *Macromolecules*, **24,** 2385.
[23] Berne, B. J., and Pecora, R., 1976, *Dynamic Light Scattering* (Wiley).
[24] Wittebrood, M. M., Rasing, T., Stallinga, S., and Musevic, I., 1998, *Phys. Rev. Lett.*, **80,** 1232.
[25] Mertelj, A., and Copic, M., 2000, *Phys. Rev. E*, **61,** 1622.
[26] Jèrôme, B., 1991, *Rep. Prog. Phys.*, **54,** 391.
[27] Clark, N. A., 1985, *Phys. Rev. Lett.*, **55,** 292.
[28] Haward, R. N., 1973, *Physics of Glassy Polymers* (New York: Elsevier).
[29] Gu, D. F., Jamieson, A. M., Lee, M.-S., Kawasumi, M., and Percec, V., 1992, *Liq. Cryst.*, **12,** 961.
[30] Benmouna, F., Peng, B., Rühe, J., and Johannsmann, D., 1999, *Liq. Cryst.*, **26,** 1655.
[31] Moses, T., and Shen, Y. R., 1991, *Phys. Rev. Lett.*, **67,** 2033.